Electronic Supplementary Material (ESI) for Lab on a Chip.

Supplementary information

Fundamentals of integrated ferrohydrodynamic cell separation in circulating tumor cells isolation

Yang Liu,[a] Wujun Zhao,[a] Rui Cheng,[b] Bryana N. Harris,[c] Kimberly Schmitz,[d] Jonathan R. Murrow,[e] Jamie Hodgson,[f] Mary Egan,[f] Anastacia Bankey,[f] Petros G. Nikolinakos,[f] Travis Laver,[g] Kristina Meichner,[h] and Leidong Mao*[b]

[a]Department of Chemistry, The University of Georgia, Athens, GA 30602, USA

[b]School of Electrical and Computer Engineering, College of Engineering, The University of Georgia, Athens, GA 30602, USA.

[c]Department of Chemical Engineering, Auburn University, Auburn, AL 36830, USA

[d]Clinical and Translational Research Unit, The University of Georgia, Athens, GA 30602, USA.

[e]Department of Medicine, Augusta University – The University of Georgia Medical Partnership, Athens, GA 30602, USA

[f]University Cancer & Blood Center, LLC, Athens, GA, 30607

[g]Small Animal Medicine and Surgery, Veterinary Teaching Hospital, The University of Georgia, Athens, GA 30602, USA.

[h]Department of Pathology, College of Veterinary Medicine, The University of Georgia, Athens, GA 30602, USA.

*E-mail: mao@uga.edu

Table. S1 A survey of existing CTC separation technologies.

Category	Type	Technique	Throughput (mL/h)	Recovery rate	Purity	Viability	Reference
Label-based	Immunoaffinity	CellSearch	N/A	~81%	N/A	N/A	1
		Magsweeper	9	59±27%	~100%	N/A	2
	Microfluidic micropost	CTC-Chip	1	>60%	~ 56%	98.5%	3
		GEDI	1	~85%	~68%	N/A	4
		OncoCEE	1	~80-90%	N/A	N/A	5
		NanoVelcro-Chip	0.5	~90%	N/A	N/A	6
	Microfluidic surface capture	HB-Chip	1.2	~91.8%	14%	95%	7
		GEM-Chip	3.6	~90%	~84%	~85%	8
		Graphene Oxide Chip	~1-3	73±2.4%	N/A	N/A	9
	Immunomagnetic positive	Ephesia-Chip	3	~90%	<100 contaminating cells	N/A	10
		Magnetic Sifter	10	48% - 90%	17.7±9.3%	N/A	11
		Isoflux	1.2	74-85%	~1.4 %	N/A	12
		CTC-iChip	8	89.7-98.6%	> 0.1 %	N/A	13
		Micromagnetic Chip	1.2	~90 %	remove > 99.6% WBC	>90%	14
		IMN	1.2	~94%	N/A	93%	15
		MAP (magnetophoresis)	10	86-90%	N/A	N/A	16
		SIM-Chip	2	82.4%	92.45%	84.1%	17
		CTC-µChip	2	~90%	15.6-35.0	N/A	18
	Immunomagnetic negative	QMS	1E6 – 1E7 cells/ s	46%	~0.1 - 6.4%	~90%	19
		EasySep™ Human CD45 Depletion Kit	N/A	69%	1%	N/A	20
		CTC-iChip	8	~ 97%	~7.8%	N/A	13
		Monolithic CTC-iChip	1.5E7 – 2E7 cells / s	~99.5%	18.4% (445 WBCs per mL)	N/A	21
		^{LP}CTC-iChip	60	86%	Remove ~99.97% WBC	N/A	22
		iFCS	**6**	**98.8%**	**~1620 WBCs per mL blood**	**97.25%**	**This work**
Label-free	Density gradient centrifugation	Ficoll-Paque	20	N/A	N/A	N/A	23
		OncoQuick	N/A	N/A	N/A	N/A	24
	Density-antibody	RosetteSep™ CTC Enrichment Cocktail	N/A	~62.5%	N/A	N/A	25
		Accucyte Enrichment and CyteSealer™	N/A	~90.5%	N/A	N/A	26
	Size-Deformability	Microfluidic Ratchet	1	~90%	Remove 99.99% WBCs	99.1%	27
		ISET®	N/A	N/A	N/A	N/A	28
		ScreenCell®	1 mL/min	74-91.2%	N/A	~85%	29
		CellSieve	2.5 mL/min	N/A	N/A	N/A	30
		FMSA	0.75 mL/min	90%	Remove 99.99% WBCs	80%	31

		SB microfilter	N/A	78-83%	Remove ~99.95% WBCs	71-74%	32
		RCT (Resettable Cell Trap)	0.6	>90%	Remove ~99.89% WBCs	N/A	33
		Cluster Chip	2.5	41-99%	~15%	~95%	34
	Inertial forces	Vortex	22.5	21%	57-94%	~86%	35
		DFF (Dean Flow Fractionation)	3	>85%	Remove ~ 99.95% WBCs	> 98%	36
	Electrophoresis	ApoStream™	~1.3	~73%	Remove ~99.99% peripheral blood mononuclear cells (PBMCs)	97.1%	37
		MOFF-DEP	7.6	75.3%	Remove 94.23% of WBCs	N/A	38
		Dielectrophoresis Device	N/A	~100% (simulation)	83% (simulation)	N/A	39
		ODEP		41.5%	~100%	N/A	40
	Acoustophoresis	taSSAW-Chip	1.2	~83%	Remove >90% WBCs	~91%	41
		Acoustophoresis Chip	6	~95%	~97.8	N/A	42
	Ferrohydrodynamics	FCS	6	~92.9%	11.7%	96.3%	43

Solving cell trajectories in iFCS.

The three-dimensional expression of the net magnetic force on a magnetizable body in a magnetizable fluid (ferrofluid) is given in the main text

$$\vec{\mathbf{F}}_{\mathbf{m}} = -\mu_0 V \left\{ \left(\vec{\mathbf{M}}_{\mathbf{ferrofluid}} - \vec{\mathbf{M}}_{\mathbf{particle}} \right) \cdot \nabla \right\} \vec{\mathbf{H}} \tag{S1}$$

In three-dimensional space, we have

$$F_{m,x} = -\mu_0 V \left[\left(M_{f,x} - M_{p,x} \right) \frac{\partial H_x}{\partial x} + \left(M_{f,y} - M_{p,y} \right) \frac{\partial H_x}{\partial y} + \left(M_{f,z} - M_{p,z} \right) \frac{\partial H_x}{\partial z} \right] \tag{S2}$$

$$F_{m,y} = -\mu_0 V \left[\left(M_{f,x} - M_{p,x} \right) \frac{\partial H_y}{\partial x} + \left(M_{f,y} - M_{p,y} \right) \frac{\partial H_y}{\partial y} + \left(M_{f,z} - M_{p,z} \right) \frac{\partial H_y}{\partial z} \right] \tag{S3}$$

$$F_{m,z} = -\mu_0 V \left[\left(M_{f,x} - M_{p,x} \right) \frac{\partial H_z}{\partial x} + \left(M_{f,y} - M_{p,y} \right) \frac{\partial H_z}{\partial y} + \left(M_{f,z} - M_{p,z} \right) \frac{\partial H_z}{\partial z} \right] \tag{S4}$$

where $F_{m,x}$, $F_{m,y}$ and $F_{m,y}$ are the *x*, *y* and *z* components of the magnetic force vector. $M_{f,x}$, $M_{f,y}$ and $M_{f,z}$ are the *x*, *y* and *z* components of the ferrofluid magnetization vector. $M_{p,x}$, $M_{p,y}$ and $M_{p,z}$ are the *x*, *y* and *z* components of the particle magnetization vector. H_x , H_y and H_z are the *x*, *y* and *z* components of the magnetic field strength vector.

The magnetic force $\vec{\mathbf{F}}_{\mathbf{m}}$ acting on the cell is balanced by the hydrodynamic viscous drag force $\vec{\mathbf{F}}_{\mathbf{d}}$, when there is a relative motion between the cell and the fluid flow. Its expression is,

$$\vec{\mathbf{F}}_{\mathbf{d}} = -3\pi\eta D_p \left(\vec{\mathbf{v}}_p - \vec{\mathbf{v}}_f \right) \lambda \tag{S5}$$

Where η is the ferrofluid viscosity, D_p is the diameter of a spherical object, $\vec{\mathbf{v}}_p$ and $\vec{\mathbf{v}}_f$ are the velocity vectors of the ferrofluid and the object. λ includes the parallel ($\lambda_{\parallel}$) and perpendicular ($\lambda_{\perp}$) components of the hydrodynamic drag force coefficient of a moving object after taking into account the influence from one nearby flat surface.[44, 45] Its appearance indicates increased fluid viscosity as the object moves closer to the solid surface.

$$\lambda_{\parallel} = \left[1 - \frac{9}{16}\left(\frac{D_p}{D_p + 2\Delta}\right) + \frac{1}{8}\left(\frac{D_p}{D_p + 2\Delta}\right)^3 - \frac{45}{256}\left(\frac{D_p}{D_p + 2\Delta}\right)^4 - \frac{1}{16}\left(\frac{D_p}{D_p + 2\Delta}\right)\right]^{-1} \tag{S6}$$

$$\lambda_{\perp} = \left[1 - \frac{9}{8}\left(\frac{D_p}{D_p + 2\Delta}\right) + \frac{1}{2}\left(\frac{D_p}{D_p + 2\Delta}\right)^3\right]^{-1} \tag{S7}$$

where Δ is the shortest distance between the solid surface and the surface of the object.

In three-dimensional space, we have

$$F_{d,x} = -3\pi\eta D_p \left(v_{p,x} - v_{f,x}\right)\lambda_{\parallel} \tag{S8}$$

$$F_{d,y} = -3\pi\eta D_p \left(v_{p,y} - v_{f,y}\right)\lambda_{\parallel} \tag{S9}$$

$$F_{d,z} = -3\pi\eta D_p \left(v_{p,z} - v_{f,z}\right)\lambda_{\perp} \tag{S10}$$

The balance of Eqs.(S1) and (S5) under laminar flow condition at low Reynold's number was used to predict the trajectories of magnetizable cells.

$$\vec{\mathbf{F}}_{\mathbf{m}} + \vec{\mathbf{F}}_{\mathbf{d}} = 0 \tag{S11}$$

which yields

$$\begin{bmatrix} v_{p,x} \\ v_{p,y} \\ v_{p,z} \end{bmatrix} = \begin{bmatrix} v_{f,x} \\ 0 \\ 0 \end{bmatrix} - \frac{\mu_0 D_p^2}{18\eta} \begin{pmatrix} \frac{1}{\lambda_{\parallel}}\left(\left(M_{f,x} - M_{p,x}\right)\frac{\partial H_x}{\partial x} + \left(M_{f,y} - M_{p,y}\right)\frac{\partial H_x}{\partial y} + \left(M_{f,z} - M_{p,z}\right)\frac{\partial H_x}{\partial z} \right) \\ \frac{1}{\lambda_{\parallel}}\left(\left(M_{f,x} - M_{p,x}\right)\frac{\partial H_y}{\partial x} + \left(M_{f,y} - M_{p,y}\right)\frac{\partial H_y}{\partial y} + \left(M_{f,z} - M_{p,z}\right)\frac{\partial H_y}{\partial z} \right) \\ \frac{1}{\lambda_{\perp}}\left(\left(M_{f,x} - M_{p,x}\right)\frac{\partial H_z}{\partial x} + \left(M_{f,y} - M_{p,y}\right)\frac{\partial H_z}{\partial y} + \left(M_{f,z} - M_{p,z}\right)\frac{\partial H_z}{\partial z} \right) \end{pmatrix}$$

(S12)

where we assume the magnetizable body is spherical and $V = \frac{1}{6}\pi D_p^3$. $v_{f,x}$ in Eq. (S12) is the ferrofluid velocity profile of a fully developed laminar flow in a rectangular microchannel (see Figure 1F in main text for coordinates) of width w and height h.[46, 47]

$$v_{f,x} = \frac{\pi Q}{2wh}\left(\frac{a}{b}\right) \tag{S13}$$

where Q is the sample flow rate and

$$a = \sum_{n=0}^{\infty} \frac{(-1)^n \cos\left[\frac{(2n+1)\pi z}{w}\right]}{(2n+1)^3} \left[1 - \frac{\cosh\left[\frac{(2n+1)\pi y}{w}\right]}{\cosh\left[\frac{(2n+1)\pi h}{2w}\right]} \right] \tag{S14}$$

$$b = \sum_{n=0}^{\infty} \frac{1}{(2n+1)^4} \left[1 - \frac{\tanh\left[\frac{(2n+1)\pi h}{2w}\right]}{\frac{(2n+1)\pi h}{2w}} \right] \tag{S15}$$

Eq. (S12) is a coupled ordinary differential equation (ode) system for the cell trajectory. We used an ode solver (ode45) in MATLAB to solve this system.

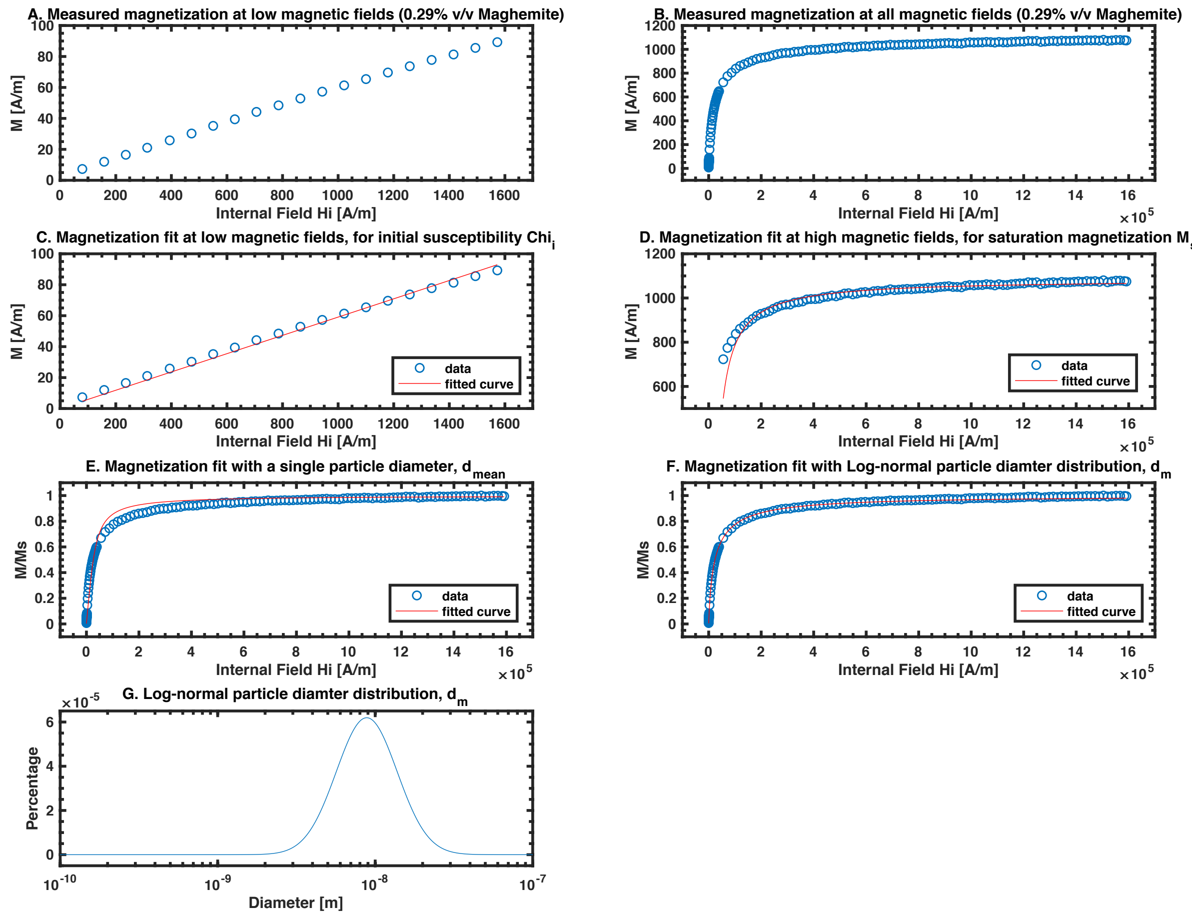

Figure S1. Experimental magnetization curve and fitted Langevin function of a maghemite ferrofluid used in this study. Temperature was 298 Kelvin, bulk magnetization of maghemite M_d was 370,000 A/m, density of the ferrofluid was 1060.6 kg/m^3, demagnetization factor due to the sample holder of the vibrating sampling magnetometer was 0.211. (A). Low field magnetization. (B). Full magnetization curve. (C). Fitted data at low field magnetization yielded an initial susceptibility χ_i of 0.0591. (D). Fitted data at high field magnetization yielded a saturation magnetization M_s of 1,085 A/m, which corresponded to a volume fraction ϕ of 0.029 of magnetic materials in this ferrofluid. (E). Fitted data of the magnetization curve with a single particle diameter yielded a diameter of 10.5 nm. (F)&(G). Fitted data of the magnetization curve with a Log-normal distribution of particle diameters yielded a volume-weighted median magnetic nanoparticle diameter D_{mv} of 10.8 nm, and a geometric standard deviation of the magnetic nanoparticle diameter distribution $\ln\sigma$ of 0.44.

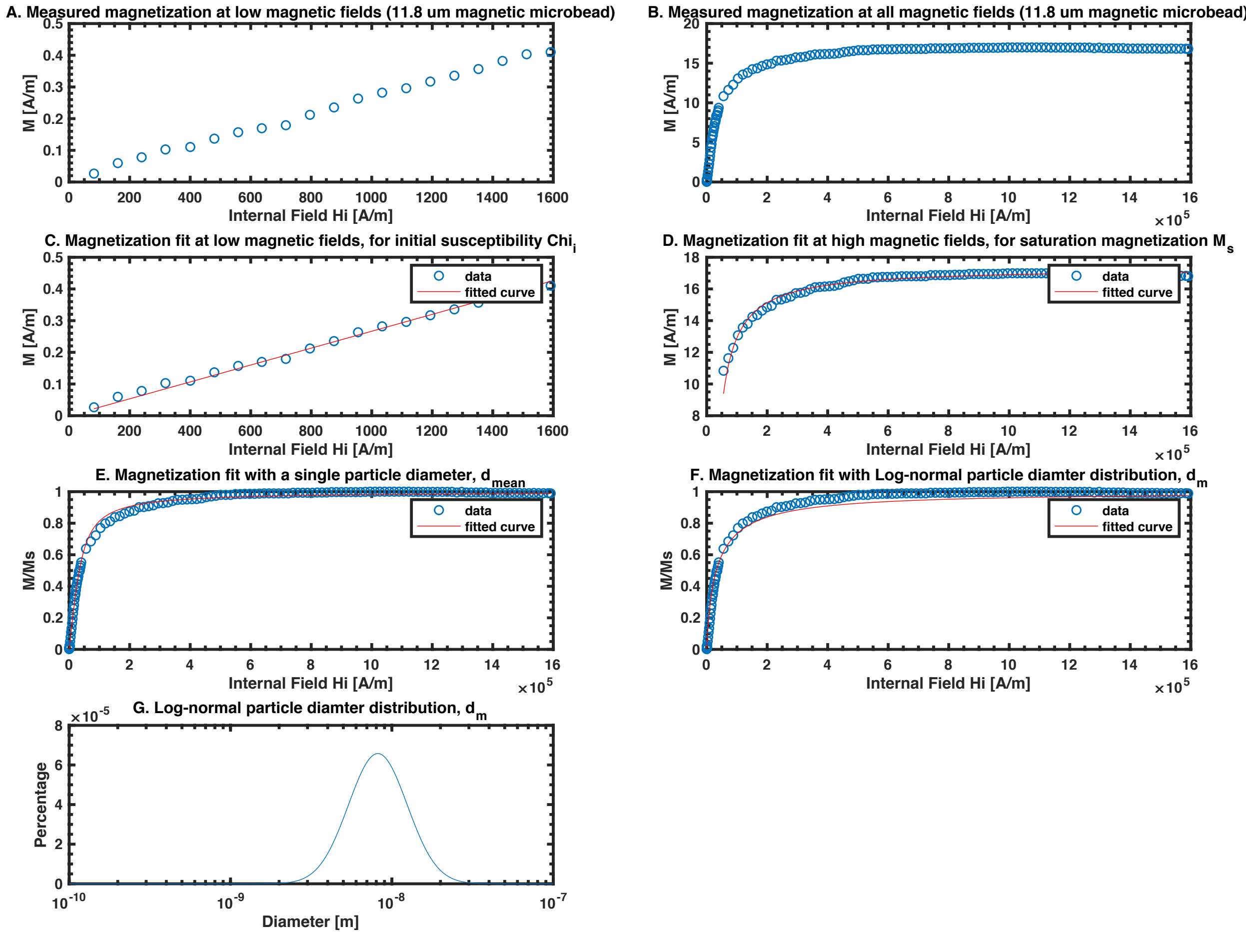

Figure S2. Experimental magnetization curve and fitted Langevin function of a 11.8 um commercial magnetic microbeads (Spherotech Inc, Lake Forest, IL) used in this study. Temperature was 298 Kelvin, bulk magnetization of maghemite M_d was 370,000 A/m, density of the microbeads was 1053.4 kg/m^3, demagnetization factor due to the sample holder of the vibrating sampling magneto-meter was 0.211. (A). Low field magnetization. (B). Full magnetization curve. (C). Fitted data at low field magnetization yielded an initial susceptibility χ_i of 0.000267. (D). Fitted data at high field magnetization yielded a saturation magnetization M_s of 17.3 A/m, which corresponded to a volume fraction ϕ of 0.0073 of magnetic materials in this microbead. (E). Fitted data of the magnetization curve with a single particle diameter yielded a diameter of 9.6 nm. (F)&(G). Fitted data of the magnetization curve with a Log-normal distribution of particle diameters yielded a volume-weighted median magnetic nanoparticle diameter D_{mv} of 9.8 nm, and a geometric standard deviation of the magnetic nanoparticle diameter distribution $\ln\sigma$ of 0.42.

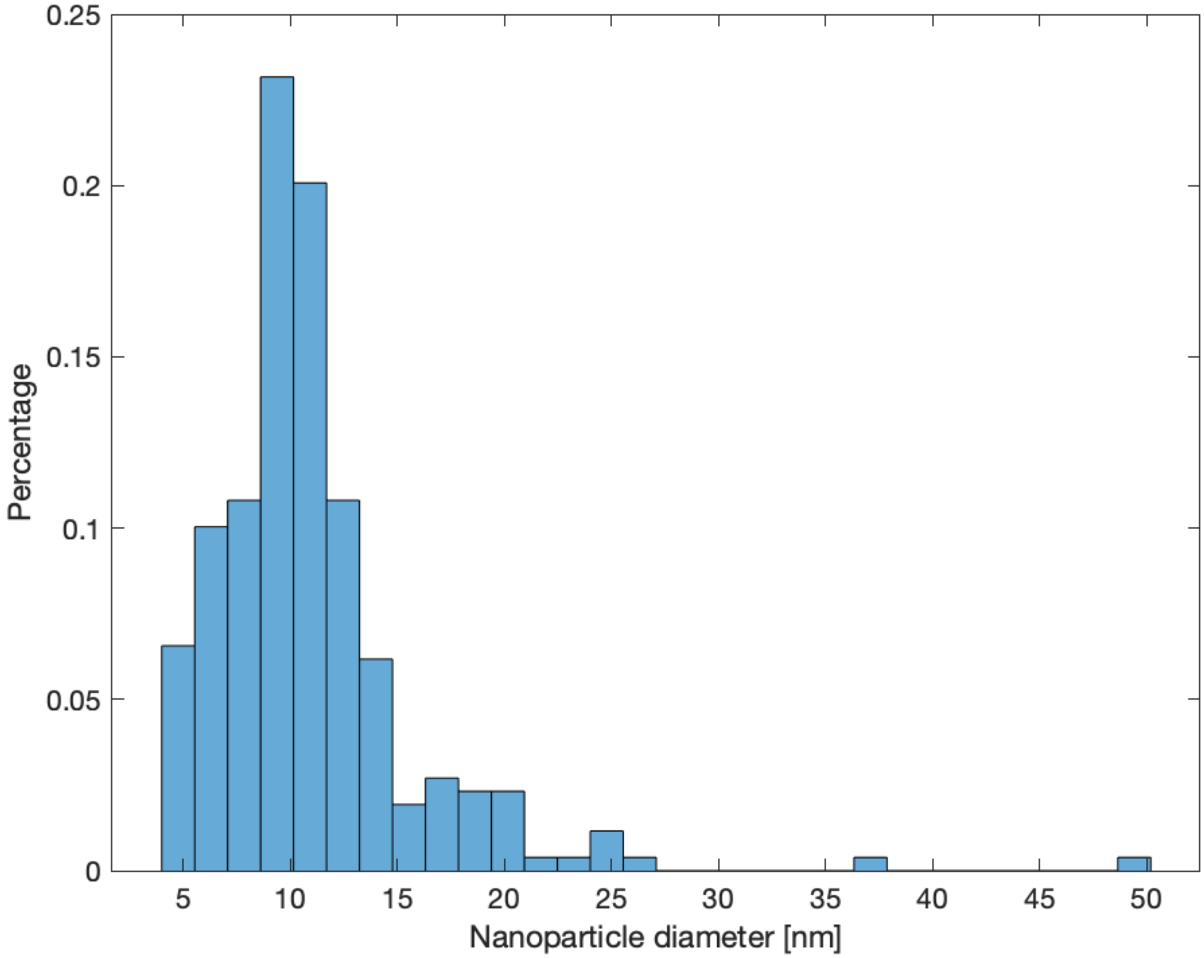

Figure S3. Particle size distribution in the maghemite ferrofluid used in this study. Transmission electron microscopy (TEM) measurement of 259 particles yielded a diameter distribution of 10.91 ± 4.87 nm.

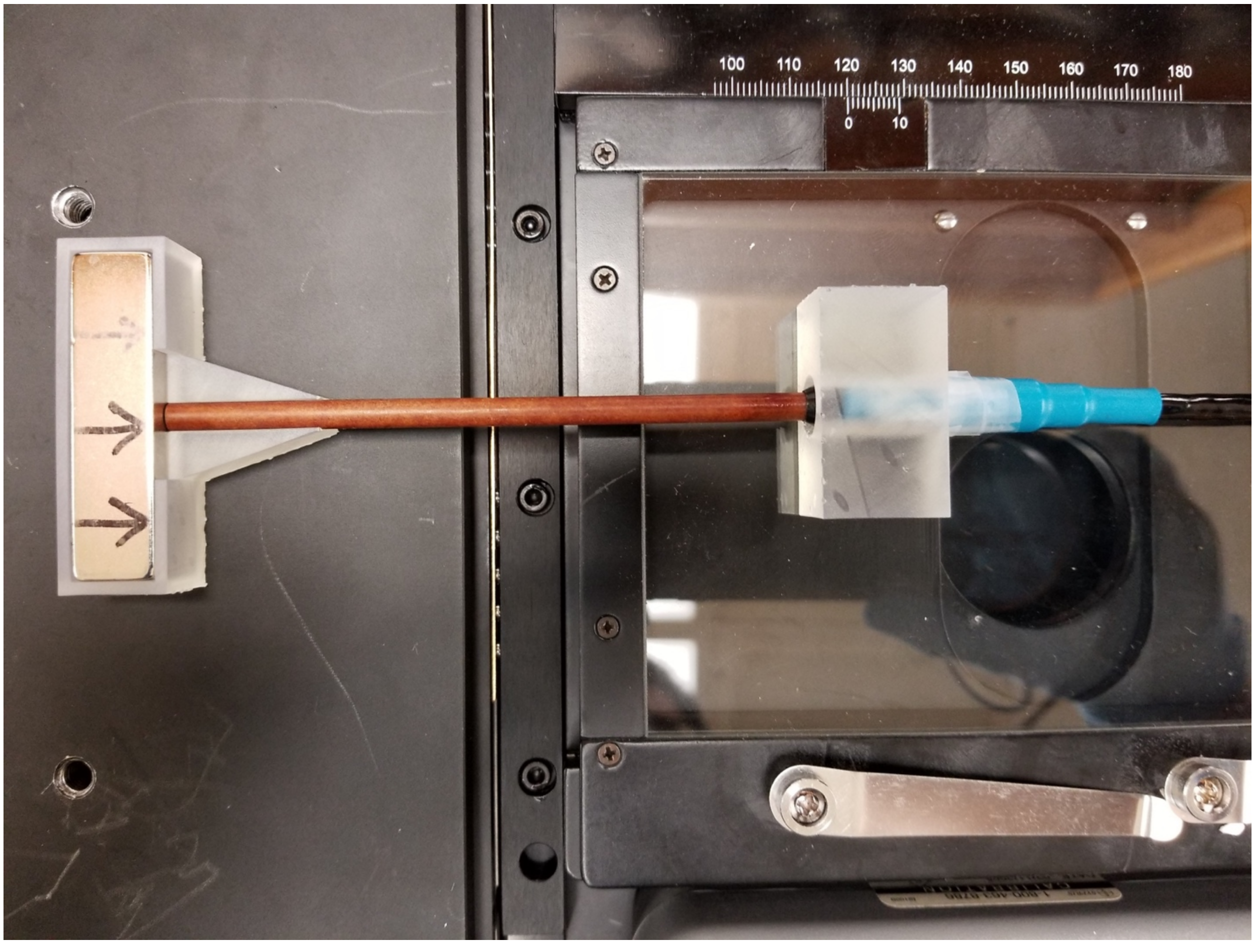

Figure S4. Experimental set up for the measurement of magnetic flux density of a neodymium permanent magnet used in the iFCS device. A Gauss meter with an axial probe was used to measure the magnetic flux density.

References:

1. S. Riethdorf, H. Fritsche, V. Muller, T. Rau, C. Schindibeck, B. Rack, W. Janni, C. Coith, K. Beck, F. Janicke, S. Jackson, T. Gornet, M. Cristofanilli and K. Pantel, *Clin Cancer Res*, 2007, **13**, 920-928.

2. A. H. Talasaz, A. A. Powell, D. E. Huber, J. G. Berbee, K. H. Roh, W. Yu, W. Z. Xiao, M. M. Davis, R. F. Pease, M. N. Mindrinos, S. S. Jeffrey and R. W. Davis, *P Natl Acad Sci USA*, 2009, **106**, 3970-3975.

3. S. Nagrath, L. V. Sequist, S. Maheswaran, D. W. Bell, D. Irimia, L. Ulkus, M. R. Smith, E. L. Kwak, S. Digumarthy, A. Muzikansky, P. Ryan, U. J. Balis, R. G. Tompkins, D. A. Haber and M. Toner, *Nature*, 2007, **450**, 1235-U1210.

4. J. P. Gleghorn, E. D. Pratt, D. Denning, H. Liu, N. H. Bander, S. T. Tagawa, D. M. Nanus, P. A. Giannakakou and B. J. Kirby, *Lab on a Chip*, 2010, **10**, 27-29.

5. S. D. Mikolajczyk, L. S. Millar, P. Tsinberg, S. M. Coutts, M. Zomorrodi, T. Pham, F. Z. Bischoff and T. J. Pircher, *Journal of Oncology*, 2011, DOI: Artn 252361
10.1155/2011/252361.

6. Y. T. Lu, L. B. Zhao, Q. L. Shen, M. A. Garcia, D. X. Wu, S. Hou, M. Song, X. C. Xu, W. H. OuYang, W. W. L. OuYang, J. Lichterman, Z. Luo, X. Xuan, J. T. Huang, L. W. K. Chung, M. Rettig, H. R. Tseng, C. Shao and E. M. Posadas, *Methods*, 2013, **64**, 144-152.

7. S. L. Stott, C. H. Hsu, D. I. Tsukrov, M. Yu, D. T. Miyamoto, B. A. Waltman, S. M. Rothenberg, A. M. Shah, M. E. Smas, G. K. Korir, F. P. Floyd, A. J. Gilman, J. B. Lord, D. Winokur, S. Springer, D. Irimia, S. Nagrath, L. V. Sequist, R. J. Lee, K. J. Isselbacher, S. Maheswaran, D. A. Haber and M. Toner, *Proceedings of the National Academy of Sciences of the United States of America*, 2010, **107**, 18392-18397.

8. W. A. Sheng, O. O. Ogunwobi, T. Chen, J. L. Zhang, T. J. George, C. Liu and Z. H. Fan, *Lab on a Chip*, 2014, **14**, 89-98.

9. H. J. Yoon, T. H. Kim, Z. Zhang, E. Azizi, T. M. Pham, C. Paoletti, J. Lin, N. Ramnath, M. S. Wicha, D. F. Hayes, D. M. Simeone and S. Nagrath, *Nat Nanotechnol*, 2013, **8**.

10. J. Autebert, B. Coudert, J. Champ, L. Saias, E. T. Guneri, R. Lebofsky, F. C. Bidard, J. Y. Pierga, F. Farace, S. Descroix, L. Malaquin and J. L. Viovy, *Lab on a Chip*, 2015, **15**, 2090-2101.

11. C. M. Earhart, C. E. Hughes, R. S. Gaster, C. C. Ooi, R. J. Wilson, L. Y. Zhou, E. W. Humke, L. Y. Xu, D. J. Wong, S. B. Willingham, E. J. Schwartz, I. L. Weissman, S. S. Jeffrey, J. W. Neal, R. Rohatgi, H. A. Wakeleebe and S. X. Wang, *Lab on a Chip*, 2014, **14**, 78-88.

12. W. Harb, A. Fan, T. Tran, D. C. Danila, D. Keys, M. Schwartz and C. Ionescu-Zanetti, *Transl Oncol*, 2013, **6**, 528-+.

13. E. Ozkumur, A. M. Shah, J. C. Ciciliano, B. L. Emmink, D. T. Miyamoto, E. Brachtel, M. Yu, P. I. Chen, B. Morgan, J. Trautwein, A. Kimura, S. Sengupta, S. L. Stott, N. M. Karabacak, T. A. Barber, J. R. Walsh, K. Smith, P. S. Spuhler, J. P. Sullivan, R. J. Lee, D. T. Ting, X. Luo, A. T. Shaw, A. Bardia, L. V. Sequist, D. N. Louis, S. Maheswaran, R. Kapur, D. A. Haber and M. Toner, *Sci Transl Med*, 2013, **5**.

14. J. H. Kang, S. Krause, H. Tobin, A. Mammoto, M. Kanapathipillai and D. E. Ingber, *Lab Chip*, 2012, **12**, 2175-2181.

15. M. Tang, C. Y. Wen, L. L. Wu, S. L. Hong, J. Hu, C. M. Xu, D. W. Pang and Z. L. Zhang, *Lab on a Chip*, 2016, **16**, 1214-1223.

16. K. Hoshino, Y. Y. Huang, N. Lane, M. Huebschman, J. W. Uhr, E. P. Frenkel and X. J. Zhang, *Lab on a Chip*, 2011, **11**, 3449-3457.

17. J. Kim, H. Cho, S.-I. Han and K.-H. Han, *Analytical chemistry*, 2016, **88**, 4857-4863.

18. H. Cho, J. Kim, C.-W. Jeon and K.-H. Han, *Lab on a Chip*, 2017, **17**, 4113-4123.

19. O. Lara, X. D. Tong, M. Zborowski and J. J. Chalmers, *Experimental Hematology*, 2004, **32**, 891-904.

20. Z. A. Liu, A. Fusi, E. Klopocki, A. Schmittel, I. Tinhofer, A. Nonnenmacher and U. Keilholz, *J Transl Med*, 2011, **9**.

21. F. Fachin, P. Spuhler, J. M. Martel-Foley, J. F. Edd, T. A. Barber, J. Walsh, M. Karabacak, V. Pai, M. Yu, K. Smith, H. Hwang, J. Yang, S. Shah, R. Yarmush, L. V. Sequist, S. L. Stott, S. Maheswaran, D. A. Haber, R. Kapur and M. Toner, *Sci Rep-Uk*, 2017, **7**.

22. A. Mishra, T. D. Dubash, J. F. Edd, M. K. Jewett, S. G. Garre, N. M. Karabacak, D. C. Rabe, B. R. Mutlu, J. R. Walsh and R. Kapur, *Proceedings of the National Academy of Sciences*, 2020, **117**, 16839-16847.

23. J. Weitz, P. Kienle, J. Lacroix, F. Willeke, A. Benner, T. Lehnert, C. Herfarth and M. von Knebel Doeberitz, *Clin Cancer Res*, 1998, **4**, 343-348.

24. G. A. Clawson, E. Kimchi, S. D. Patrick, P. Xin, R. Harouaka, S. Zheng, A. Berg, T. Schell, K. F. Staveley-O'Carroll, R. I. Neves, P. J. Mosca and D. Thiboutot, *PLoS One*, 2012, **7**, e41052.

25. W. He, S. A. Kularatne, K. R. Kalli, F. G. Prendergast, R. J. Amato, G. G. Klee, L. C. Hartmann and P. S. Low, *Int J Cancer*, 2008, **123**, 1968-1973.

26. D. E. Campton, A. B. Ramirez, J. J. Nordberg, N. Drovetto, A. C. Clein, P. Varshavskaya, B. H. Friemel, S. Quarre, A. Breman, M. Dorschner, S. Blau, C. A. Blau, D. E. Sabath, J. L. Stilwell and E. P. Kaldjian, *BMC Cancer*, 2015, **15**, 360.

27. E. S. Park, C. Jin, Q. Guo, R. R. Ang, S. P. Duffy, K. Matthews, A. Azad, H. Abdi, T. Todenhöfer and J. Bazov, *Small*, 2016, **12**, 1909-1919.

28. G. Vona, A. Sabile, M. Louha, V. Sitruk, S. Romana, K. Schutze, F. Capron, D. Franco, M. Pazzagli, M. Vekemans, B. Lacour, C. Brechot and P. Paterlini-Brechot, *Am J Pathol*, 2000, **156**, 57-63.

29. I. Desitter, B. S. Guerrouahen, N. Benali-Furet, J. Wechsler, P. A. Janne, Y. Kuang, M. Yanagita, L. Wang, J. A. Berkowitz, R. J. Distel and Y. E. Cayre, *Anticancer Res*, 2011, **31**, 427-441.

30. D. L. Adams, S. S. Martin, R. K. Alpaugh, M. Charpentier, S. Tsai, R. C. Bergan, I. M. Ogden, W. Catalona, S. Chumsri, C.-M. Tang and M. Cristofanilli, 2014, DOI: 10.1073/pnas.1320198111 %J Proceedings of the National Academy of Sciences, 201320198.

31. R. A. Harouaka, M. D. Zhou, Y. T. Yeh, W. J. Khan, A. Das, X. Liu, C. C. Christ, D. T. Dicker, T. S. Baney, J. T. Kaifi, C. P. Belani, C. I. Truica, W. S. El-Deiry, J. P. Allerton and S. Y. Zheng, *Clin Chem*, 2014, **60**, 323-333.

32. M. D. Zhou, S. Hao, A. J. Williams, R. A. Harouaka, B. Schrand, S. Rawal, Z. Ao, R. Brenneman, E. Gilboa, B. Lu, S. Wang, J. Zhu, R. Datar, R. Cote, Y. C. Tai and S. Y. Zheng, *Sci Rep*, 2014, **4**, 7392.

33. X. Qin, S. Park, S. P. Duffy, K. Matthews, R. R. Ang, T. Todenhofer, H. Abdi, A. Azad, J. Bazov, K. N. Chi, P. C. Black and H. Ma, *Lab Chip*, 2015, **15**, 2278-2286.

34. A. F. Sarioglu, N. Aceto, N. Kojic, M. C. Donaldson, M. Zeinali, B. Hamza, A. Engstrom, H. Zhu, T. K. Sundaresan, D. T. Miyamoto, X. Luo, A. Bardia, B. S. Wittner, S. Ramaswamy, T. Shioda, D. T. Ting, S. L. Stott, R. Kapur, S. Maheswaran, D. A. Haber and M. Toner, *Nat Methods*, 2015, **12**, 685-691.

35. E. Sollier, D. E. Go, J. Che, D. R. Gossett, S. O'Byrne, W. M. Weaver, N. Kummer, M. Rettig, J. Goldman, N. Nickols, S. McCloskey, R. P. Kulkarni and D. Di Carlo, *Lab Chip*, 2014, **14**, 63-77.

36. H. W. Hou, M. E. Warkiani, B. L. Khoo, Z. R. Li, R. A. Soo, D. S. Tan, W. T. Lim, J. Han, A. A. Bhagat and C. T. Lim, *Sci Rep*, 2013, **3**, 1259.

37. V. Gupta, I. Jafferji, M. Garza, V. O. Melnikova, D. K. Hasegawa, R. Pethig and D. W. Davis, *Biomicrofluidics*, 2012, **6**, 24133.

38. H.-S. Moon, K. Kwon, S.-I. Kim, H. Han, J. Sohn, S. Lee and H.-I. Jung, *Lab on a Chip*, 2011, **11**, 1118-1125.

39. V. Shirmohammadli and N. Manavizadeh, *IEEE Transactions on Electron Devices*, 2019, **66**, 4075-4080.

40. T.-K. Chiu, W.-P. Chou, S.-B. Huang, H.-M. Wang, Y.-C. Lin, C.-H. Hsieh and M.-H. Wu, *Sci Rep-Uk*, 2016, **6**, 1-14.

41. P. Li, Z. Mao, Z. Peng, L. Zhou, Y. Chen, P. H. Huang, C. I. Truica, J. J. Drabick, W. S. El-Deiry, M. Dao, S. Suresh and T. J. Huang, *Proc Natl Acad Sci U S A*, 2015, **112**, 4970-4975.

42. M. Antfolk, C. Antfolk, H. Lilja, T. Laurell and P. Augustsson, *Lab Chip*, 2015, **15**, 2102-2109.

43. W. Zhao, R. Cheng, B. D. Jenkins, T. Zhu, N. E. Okonkwo, C. E. Jones, M. B. Davis, S. K. Kavuri, Z. Hao, C. Schroeder and L. Mao, *Lab Chip*, 2017, **17**, 3097-3111.

44. H. Brenner, *Chem Eng Sci*, 1961, **16**, 242-251.

45. B. H. Lin, J. Yu and S. A. Rice, *Phys Rev E*, 2000, **62**, 3909-3919.

46. N. Ichikawa, K. Hosokawa and R. Maeda, *Journal of Colloid and Interface Science*, 2004, **280**, 155-164.

47. J. P. Brody, P. Yager, R. E. Goldstein and R. H. Austin, *Biophysical Journal*, 1996, **71**, 3430-3441.